Structural Optimization of Biomorphic Microcellular Ceramics by Homogenization Approach

Ronald H.W. Hoppe[1] and Svetozara I. Petrova[2]

[1] Institute of Mathematics, University of Augsburg,
Universitystr.14, D-86159 Augsburg, Germany
[2] Central Laboratory for Parallel Processing, Bulgarian Academy of Sciences,
Acad. G. Bontchev Str., Block 25A, 1113 Sofia, Bulgaria

Abstract. For the last decade material synthesis from biological structures has become of increasing interest. Various biotemplating high–temperature techniques were developed to convert natural grown materials into ceramic and composite materials. A new class of structural materials, biomorphic microcellular silicon carbide ceramics from wood, was recently technically produced. It could be of particular interest for applications in acoustic and heat insulation structures. In the attempt to optimize mechanical performances of the microstructured ceramic composites such as the compliance or the bending strength, we have applied the homogenization method. The macroscale model was obtained assuming a periodical distribution of the composite microstructure with a square periodicity cell.

1 Introduction

Biotemplating is a novel technology of biomimetic processing which has in the last years attracted a lot of attention. Various biotemplating high–temperature techniques were developed to convert natural grown materials into ceramic and composite materials. Among the major classes of such ceramic composites, new biomorphic cellular silicon carbide (SiC) ceramics from wood were recently produced and investigated (see Fig. 1 and c.f., e.g., [4,5]). The new ceramic materials can not be considered furthermore as wood but have a unique oriented cellular microstructure pseudomorphous to wood. Depending on the initial cellular microstructure of various kinds of wood, ceramic materials of different density, pore structure, and degree of anisotropy were obtained.

The preparation of the SiC ceramic materials includes a two–step process: preprocessing (shaping, drying, high–temperature pyrolysis) followed by a liquid

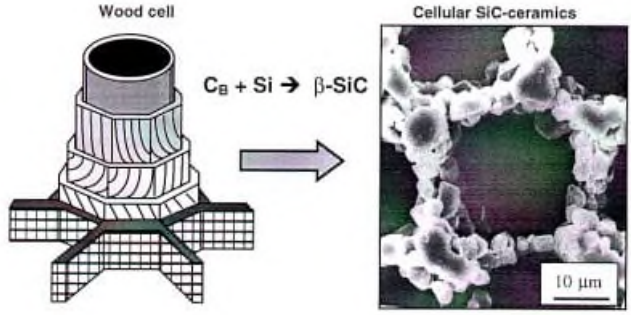

Fig. 1. Basic principles of biotemplating: Conversion of bioorganic carbon structures into ceramic composites by high–temperature processing.

or gaseous infiltration of silicon (Si) at high temperature. More precisely, natural wood of different pore size distribution and composition was carbonized at 800–1800°C for four hours in inert atmosphere resulting in a one–to–one reproduction of the original wood structure. Afterwards, the obtained porous carbon preform was infiltrated with liquid or gaseous silicon (Si–melt or Si–gas, respectively) at 1600°C in vacuum and converted to inorganic, porous SiC ceramic material. Fig.2 shows the conversion of pine wood into a microcellular SiC–ceramic. The reaction with gaseous Si–infiltrants results in ceramic composite structures with a larger porosity but the processing is more time–consuming than by using Si–melt infiltration. The processing of pyrolysis, infiltration, and reaction was described in detail in [4].

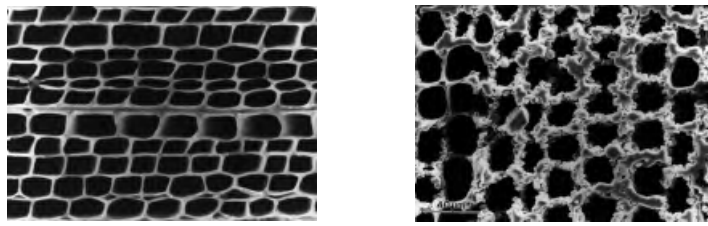

Fig. 2. Cellular β-SiC ceramic derived from wood: a) pyrolized pine template, b) Si–gas infiltrated pine (pyrolysis + infiltration at 1600^o in Ar atmosphere).

Strength and elastic modulus of the pyrolyzed carbon preform and of the final SiC ceramic were derived from stress–strain measurements in different loading directions (e.g., axial, radial, and tangential). The molecular orientation of the carbon induces a crystallographic texture of the SiC composite which strongly influences the mechanical and elastical properties of the ceramic materials. We assume a periodical distribution of the microstructure with a square tracheidal

periodicity cell. The macroscopic scale model was designed by using the homogenization method which has found a lot of important applications in mechanics of composite materials (cf., e.g., [1,3,6,7]).

The shape and the topology of the microstructure have a significant impact on the macroscopic mechanical properties, so that the optimal structural design of microstructured materials is one of the central issues of material science (cf., e.g., [2] and the references therein). Our main aim is to develop efficient tools for the structural optimization of biomorphic microcellular ceramics based on homogenization modelling. The paper focuses on some first results in this field organized as follows. In Section 2 we introduce the primal–dual formulation of our nonlinear nonconvex optimization problem based on the classical logarithmic barrier functions. Section 3 describes the problem of computing the mechanical quantities like deformations and stresses of the biomorphic microcellular ceramics both in local (microscopic) and macroscopic regime. The macroscopic homogenized model was obtained assuming an asymptotic expansion of the solution of the nonhomogenized elasticity equation with a scale parameter close to zero. Note that the computation of the effective properties plays a key role for the structural optimization since the homogenized equation is considered as an equality constraint in the optimization problem.

2 The Structural Optimization Problem

We attempt to optimize mechanical properties of the ceramic composites such as the compliance or the bending strength taking into account technological and problem specific constraints on the *state variables* and *design parameters*. For recent results on optimal design of mechanical structures described by continuum mechanical models we refer to [2].

The design objective is to optimize a merit functional

$$\inf_{\mathbf{u},\boldsymbol{\alpha}} J(\mathbf{u};\boldsymbol{\alpha}) \ , \qquad \boldsymbol{\alpha} := (\alpha_1, \ldots, \alpha_m) \ , \tag{1}$$

subject to equality and inequality constraints

$$c(\mathbf{u},\boldsymbol{\alpha}) = 0 \ , \qquad d(\mathbf{u},\boldsymbol{\alpha}) \geq 0 \ , \tag{2}$$

for the state variables $\mathbf{u}$ and the design parameters $\alpha_i,\ 1 \leq i \leq m$. Here, $\mathbf{u}$ stands for the displacement vector whereas the design parameters reflect both the microstructure in terms of the angles and diameters of the tracheidal cells and the width of the cell walls (see Fig.3) as well as macroscopic physical quantities such as the density. The objective functional J is chosen as the compliance (maximum global stiffness).

The primal–dual nonlinear interior–point approach to the optimization problem (1) in discrete formulation relies on the substitution of the inequality constraints in (2) by logarithmic barrier functions and results in the parametrized family of optimization subproblems

$$\inf_{\mathbf{u_h},\boldsymbol{\alpha_h}} [J(\mathbf{u_h};\boldsymbol{\alpha_h}) - \rho \sum_j \log d_j(\mathbf{u_h},\boldsymbol{\alpha_h})] \ , \qquad \rho > 0 \ , \tag{3}$$

under the equality constraints

$$A_h(\boldsymbol{\alpha_h})\,\mathbf{u_h} = \mathbf{f_h}\ , \qquad c(\mathbf{u_h}, \boldsymbol{\alpha_h}) = \mathbf{0}\ , \tag{4}$$

where the first constraint in (4) stands for the discrete homogenized equation. Coupling the equality constraints (4) by Lagrangian multipliers $\boldsymbol{\lambda}$ and $\boldsymbol{\mu}$, we are led to a saddle–point problem for the Lagrangian

$$\begin{aligned}\mathcal{L}_\rho(\mathbf{u_h}, \boldsymbol{\alpha_h}; \boldsymbol{\lambda}, \boldsymbol{\mu}) := J(\mathbf{u_h}; \boldsymbol{\alpha_h}) - \rho \sum_j \log d_j(\mathbf{u_h}, \boldsymbol{\alpha_h}) \\ + \boldsymbol{\lambda}^T (A_h(\boldsymbol{\alpha_h})\mathbf{u_h} - \mathbf{f_h}) + \boldsymbol{\mu}^T\, c(\mathbf{u_h}, \boldsymbol{\alpha_h})\ .\end{aligned} \tag{5}$$

The Karush–Kuhn–Tucker conditions associated with the saddle–point problem for the Lagrangian (5) are solved by damped Newton iterations. Modern approaches rely on primal–dual techniques using simultaneous sequential quadratic programming (SQP) for the resulting equality constrained minimization subproblems. The convergence to a local minimizer is monitored by means of one or several appropriately chosen merit functions. Within our knowledges, no work has been devoted to the optimal design of the new composite materials described in Section 1. Moreover, it is considered of utmost importance that the mathematical work is supported by experimental investigations that provide both realistic model parameters as well as data for model validation.

3 The Homogenization Technique

Let $\Omega \subset \mathbf{R}^2$ be a bounded domain occupied by a body consisting of a composite material of periodically distributed constituents. Suppose that the boundary $\partial\Omega = S_1 \cup S_2,\ S_1 \cap S_2 = \emptyset,\ \text{meas}\, S_1 > 0$. Denote the space $H := \{\boldsymbol{u} | \boldsymbol{u} \in (H^1(\Omega))^2, \boldsymbol{u}_{|_{S_1}} = \mathbf{0}\}$. We are interested in the macroscopic behavior of the composite medium in the stationary case. Let the macroscopic length be L. The local structure is assumed periodic with a square period Y of characteristic length l. Homogenization is possible if the scales are well separated, i.e., we suppose that $l \ll L$. The body in the local structure consists of void and two materials denoted on Fig.3 by V, S, and C. Here, V stands for a void, S stands for SiC (silicon carbide) medium, and C for the carbon phase.

We use both lengths L and l characterizing the macroscopic and local structures to introduce two dimensionless space variables $x = X/L$ (macroscopic variable) and $y = X/l$ (microscopic variable). Denote by $\varepsilon = x/y = l/L \ll 1$ a small parameter (dimensionless number) which will be used as a *scale parameter* in the considerations further. Note that the value of ε is small with respect to the size of Ω.

Suppose that each constituent in the cell $\alpha \in \{V, S, C\}$ is isotropic and homogeneous. For the physical space variable X we consider the following elasticity problem

$$-\operatorname{div} \boldsymbol{\sigma}(X) \ = \ \mathbf{F}(X) \qquad \text{in } Y, \tag{6}$$

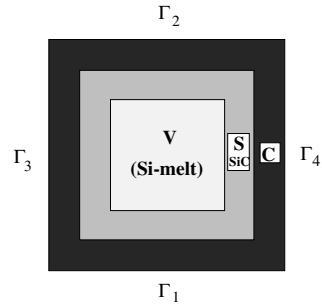

Fig. 3. The periodicity cell $Y = V \cup S \cup C$.

subjected to periodic boundary conditions imposed on $\Gamma_i,\ i = 1, \ldots, 4$ (see Fig.3) and continuity conditions $[\boldsymbol{u}] = 0$ and $[\boldsymbol{\sigma} \cdot \mathbf{n}] = 0$ on the interfaces V–S and S–C. The symbol $[*]$ denotes the jump of the function across the corresponding interface with a normal vector $\mathbf{n}$ (cf., e.g., [1]). Here, $\boldsymbol{\sigma} = (\sigma_{ij})_{i,j=1}^{2}$ is the *Cauchy stress tensor* (symmetric), $\boldsymbol{u}$ is the *displacement vector*, and $\mathbf{F}$ is related to body forces applied to Y. For simplicity, we consider the case of linear elasticity, i.e., the so–called *stress–strain state* is given by the linearized Hooke's law:

$$\boldsymbol{\sigma}_\alpha(X) = \boldsymbol{E}_\alpha \boldsymbol{e}_\alpha(\boldsymbol{u}_\alpha), \tag{7}$$

where for $\alpha \in \{V, S, C\}$, $\boldsymbol{E}_\alpha$ is the *elasticity tensor*, $\boldsymbol{e}_\alpha = (e_{\alpha\, ij})_{i,j=1}^{2}$ is the *strain tensor* (symmetric), and $\boldsymbol{u}_\alpha(X) = (u_{\alpha\,1}, u_{\alpha\,2})$ is the corresponding displacement vector. Note that in the real model the constitutive equation (7) will include in addition the plastic strain tensor and a tensor related to a lattice mismatch due to the lattice orientation between the different phases of carbon and SiC. In the case of small displacements, the linearized strain tensor $\boldsymbol{e}_\alpha(\boldsymbol{u}_\alpha) := 0.5\,(\nabla \boldsymbol{u}_\alpha + (\nabla \boldsymbol{u}_\alpha)^T)$. The stress tensor in (7) is given entrywise as $\sigma_{\alpha\, ij} = E_{\alpha\, ijkl}\, e_{\alpha\, kl} := \sum_{k,l=1}^{2} E_{\alpha\, ijkl}\, e_{\alpha\, kl}$. The *elasticity coefficients* $E_{\alpha\, ijkl}$ are supposed *Y-periodic in y*, i.e., with equal traces on the opposite sides of Y. The elasticity tensor is symmetric and verifies

$$E_{\alpha\, ijkl} = E_{\alpha\, jikl} = E_{\alpha\, ijlk} = E_{\alpha\, klij} \qquad \forall i, j, k, l = 1, 2. \tag{8}$$

Assume also that the elasticity coefficients satisfy the *ellipticity conditions*, i.e., there exist constants $\gamma_\alpha > 0$, $\alpha \in \{V, S, C\}$, such that $E_{\alpha\, ijkl}\, \xi_{ij} \xi_{kl} \geq \gamma_\alpha\, \xi_{ij}^2,\ \forall \xi_{ij} = \xi_{ji}$. For the elasticity coefficients the following relations are valid

$$\begin{gathered} E_{\alpha\,1111} = E_{\alpha\,2222} = E_\alpha/(1-\nu_\alpha^2), \quad E_{\alpha\,1122} = E_{\alpha\,2211} = \nu_\alpha E_{\alpha\,1111}, \\ E_{\alpha\,1212} = 0.5\, E_\alpha/(1+\nu_\alpha) = 0.5\,(1-\nu_\alpha) E_{\alpha\,1111}, \end{gathered} \tag{9}$$

where E_α and ν_α are *Young's modulus* and *Poisson's ratio* for $\alpha \in \{V, S, C\}$.

Denote by $\boldsymbol{u}_\varepsilon(x) := \boldsymbol{u}(x/\varepsilon)$ the unknown displacement vector in Ω. We consider now the following problem in dimensionless macroscopic description

$$-\operatorname{div} \boldsymbol{\sigma}_\varepsilon(x) = \mathbf{f}(x) \qquad \text{in } \Omega, \tag{10}$$

subjected to a macroscopic body force $\mathbf{f}$ and a macroscopic surface traction. Here, $\boldsymbol{\sigma}_\varepsilon(x) = \boldsymbol{E}_\varepsilon(x)\boldsymbol{e}(\boldsymbol{u}_\varepsilon)$ is the stress tensor and $\boldsymbol{E}_\varepsilon(x) := \boldsymbol{E}(x/\varepsilon) = \boldsymbol{E}(y)$ is the piecewise constant elasticity tensor defined on the periodicity cell Y. Note that for smaller and smaller ε, $\boldsymbol{E}_\varepsilon(x)$ oscillates more and more rapidly.

It is known (cf., e.g., [3]) that the sequence $\{\boldsymbol{u}_\varepsilon\}$ of solutions of (10) tends weakly in H as $\varepsilon \to 0$ to a vector function $\boldsymbol{u}^{(0)}(x) \in H$ which is the solution of the following elasticity problem defined in Ω with a constant elasticity tensor

$$-\operatorname{div}\boldsymbol{\sigma}(x) = \mathbf{f}(x) \qquad \text{in } \Omega. \tag{11}$$

Here, $\boldsymbol{\sigma}(x) = \boldsymbol{E}^H \boldsymbol{e}_x(\boldsymbol{u}^{(0)})$ is the so-called *homogenized stress tensor*, $\boldsymbol{E}^H$ is the *homogenized elasticity tensor* with constant components E^H_{ijkl} (called *homogenized* or *effective* coefficients), and $\boldsymbol{u}^{(0)}(x)$ is the *homogenized displacement vector*. Equation (11) is referred to as the *homogenized problem*.

We use a double scale asymptotic expansion (cf., e.g., [1,3,6]) of $\boldsymbol{u}_\varepsilon$ in the form

$$\boldsymbol{u}_\varepsilon(x) = \boldsymbol{u}^{(0)}(x,y) + \varepsilon\,\boldsymbol{u}^{(1)}(x,y) + \varepsilon^2\,\boldsymbol{u}^{(2)}(x,y) + \cdots, \tag{12}$$

where $\boldsymbol{u}^{(j)}(x,y)$ are Y-periodic in y. Since $y_i = \varepsilon^{-1}x_i$ for $i = 1,2$, we can use the following differentiation rule

$$\frac{d}{dx_i} G\left(x_i, \frac{x_i}{\varepsilon}\right) = \frac{\partial G(x_i,y_i)}{\partial x_i} + \varepsilon^{-1}\frac{\partial G(x_i,y_i)}{\partial y_i}.$$

In what follows, the subscripts x and y indicate the partial derivatives with respect to the space variables x and y, respectively. Then, the elasticity equation (10) reads

$$-\operatorname{div}_x\left(\boldsymbol{E}(y)\boldsymbol{e}_x(\boldsymbol{u}_\varepsilon)\right) = \mathbf{f}(x). \tag{13}$$

Replacing $\boldsymbol{u}_\varepsilon$ from (12) in equation (13), one gets

$$-\left(\operatorname{div}_x + \varepsilon^{-1}\operatorname{div}_y\right)\Big\{\boldsymbol{E}(y)\Big(\varepsilon^{-1}\boldsymbol{e}_y(\boldsymbol{u}^{(0)}) + \boldsymbol{e}_x(\boldsymbol{u}^{(0)}) + \boldsymbol{e}_y(\boldsymbol{u}^{(1)}) + \varepsilon(\boldsymbol{e}_x(\boldsymbol{u}^{(1)}) + \boldsymbol{e}_y(\boldsymbol{u}^{(2)})) + \varepsilon^2\boldsymbol{e}_x(\boldsymbol{u}^{(2)})\Big)\Big\} = \mathbf{f}(x).$$

Identify now the same powers of ε we arrive successively at the following problems

$$A_1\boldsymbol{u}^{(0)} = \mathbf{0}, \tag{14}$$
$$A_2\boldsymbol{u}^{(0)} + A_1\boldsymbol{u}^{(1)} = \mathbf{0}, \tag{15}$$
$$A_3\boldsymbol{u}^{(0)} + A_2\boldsymbol{u}^{(1)} + A_1\boldsymbol{u}^{(2)} = \mathbf{f}(x), \tag{16}$$

where the operators $A_i,\ i = 1,2,3$, are defined as follows

$$A_1 := -\operatorname{div}_y\left(\mathbf{E}(y)\,\mathbf{e}_y\right),$$
$$A_2 := -\operatorname{div}_y\left(\mathbf{E}(y)\,\mathbf{e}_x\right) - \operatorname{div}_x\left(\mathbf{E}(y)\,\mathbf{e}_y\right),$$
$$A_3 := -\operatorname{div}_x\left(\mathbf{E}(y)\,\mathbf{e}_x\right).$$

The solution $\boldsymbol{u}^{(0)}(x,y)$ of (14) is Y-periodic in y and $A_1\boldsymbol{u}^{(0)} = \mathbf{0}$. Hence, $\boldsymbol{u}^{(0)}(x,y)$ is independent of y, i.e., $\boldsymbol{u}^{(0)}(x,y) = \boldsymbol{u}^{(0)}(x)$. Taking into account that $\boldsymbol{e}_y(\boldsymbol{u}^{(0)}(x)) = \mathbf{0}$ the problem (15) results in

$$\mathrm{div}_y\left(\boldsymbol{E}(y)\boldsymbol{e}_x(\boldsymbol{u}^{(0)})\right) + \mathrm{div}_y\left(\boldsymbol{E}(y)\boldsymbol{e}_y(\boldsymbol{u}^{(1)})\right) = \mathbf{0}. \tag{17}$$

We look for $\boldsymbol{u}^{(1)}(x,y)$ as a linear vector function of $\boldsymbol{e}_x(\boldsymbol{u}^{(0)})$ in the form

$$\boldsymbol{u}^{(1)}(x,y) = -\boldsymbol{\xi}(y)\boldsymbol{e}_x(\boldsymbol{u}^{(0)}(x)) + \bar{\boldsymbol{u}}^{(1)}(x), \tag{18}$$

where $\bar{\boldsymbol{u}}^{(1)}(x)$ is an arbitrary function of x, $\boldsymbol{\xi}(y) = \boldsymbol{\xi}(y_1,y_2)$ is a third order tensor, y depending and periodic in each argument, i.e., $\xi_p^{kl}(y_1,y_2) \in H^1(Y)$ are supposed Y-periodic functions, $p,k,l = 1,2$. From (17) and (18) one gets

$$\mathrm{div}_y\left(\boldsymbol{E}(y) - \boldsymbol{E}(y)\boldsymbol{e}_y(\boldsymbol{\xi}^{kl})\right) = \mathbf{0}. \tag{19}$$

$\boldsymbol{\xi}(y)$ is defined up to an additive constant. For uniqueness we choose $\boldsymbol{\xi}(y)$ having zero mean value in Y, i.e., $< \boldsymbol{\xi}(y) >= 0$, where the volume average symbol is defined as $< * >:= |Y|^{-1}\int_Y * \, dY$. We solve then equation (16) to find $\boldsymbol{u}^{(2)}$. Compatibility condition for existence of $\boldsymbol{u}^{(2)}$, given by the Fredholm equality, successively yields

$$-\int_Y \mathrm{div}_x\left(\boldsymbol{E}(y)\boldsymbol{e}_x(\boldsymbol{u}^{(0)}) + \boldsymbol{E}(y)\boldsymbol{e}_y(\boldsymbol{u}^{(1)})\right)\, dy = |Y|\,\mathbf{f}(x). \tag{20}$$

Replacing (18) in (20) and taking into account that $\boldsymbol{e}_y(\bar{\boldsymbol{u}}^{(1)}(x)) = \mathbf{0}$, it holds that

$$-\mathrm{div}_x\left(\left(\int_Y (\boldsymbol{E}(y) - \boldsymbol{E}(y)\boldsymbol{e}_y(\boldsymbol{\xi}^{kl})\, dy\right)\boldsymbol{e}_x(\boldsymbol{u}^{(0)})\right) = |Y|\,\mathbf{f}(x). \tag{21}$$

Therefore, from (11) and (21), the homogenized elasticity tensor has the form $\boldsymbol{E}^H =< \boldsymbol{E}(y) - \boldsymbol{E}(y)\boldsymbol{e}_y(\boldsymbol{\xi}^{kl}) >$ which may be written in the sense of distributions as follows

$$E^H_{ijkl} = \frac{1}{|Y|}\int_Y \left(E_{ijkl}(y) - E_{ijpq}(y)\frac{\partial \xi_p^{kl}}{\partial y_q}\right)\, dy. \tag{22}$$

The homogenized elasticity coefficients E^H_{ijkl} can be obtained analytically in the case of layered materials and checkerboard structures (cf., e.g.,[1,2,7]) or numerically through a suitable micromechanical modelling.

Acknowledgments

The authors would like to express their gratitude to Prof. Stefan Müller for the helpful comments and suggestions.

This work has been partially supported by the German National Science Foundation (DFG) under Grant No.HO877/5-1. The second author has also been supported in part by the Bulgarian Ministry for Education, Science, and Technology under Grant MM–98#801.

References

1. N. Bakhvalov and G. Panasenko. *Averaging Processes in Periodic Media*, Nauka, Moscow, 1984.
2. M. P. Bendsøe. *Optimization of Structural Topology, Shape, and Material*, Springer, 1995.
3. A. Bensoussan, J. L. Lions, anf G. Papanicolaou. *Asymptotic Analysis for Periodic Structures*, North–Holland, Elsevier Science Publishers, Amsterdam, 1978.
4. P. Greil, T. Lifka, and A. Kaindl. Biomorphic cellular silicon carbide ceramics from wood: I. Processing and microstructure, *J. Europ. Ceramic Soc.*, 18, 1961–1973, 1998.
5. P. Greil, T. Lifka, and A. Kaindl. Biomorphic cellular silicon carbide ceramics from wood: II. Mechanical properties, *J. Europ. Ceramic Soc.*, 18, 1975–1983, 1998.
6. U. Hornung. *Homogenization and Porous Media*, Springer, 1997.
7. V. V. Jikov, S. M. Kozlov, and O. A. Oleinik. *Homogenization of Differential Operators and Integral Functionals*, Springer, 1994.